

Verification of the Effect of Design Parameters on the Radius of Curvature of Vine-Like, Power Soft Gripper

Hiroto Kodama¹, Hiroyuki Nabae¹, Gen Endo¹, and Koichi Suzumori¹

Abstract— We are developing a vine-Like, power soft gripper based on Euler’s belt theory to achieve high load capacity for grasping irregularly shaped heavy objects at disaster sites. This gripper consists of a fire hose with rubber sheets adhered to both sides and a spiral constant-force spring inserted inside. Initially coiled in a helical shape, it extends while increasing its radius of curvature when air pressure is applied. In this state, it approaches the target object and wraps around it when depressurized. Therefore, the inner diameter of the gripper in its initial state determines the minimum diameter of the object that can be grasped. Additionally, at present, the radius of curvature is small when pressurized, limiting its range of motion and restricting the objects it can grasp and its use in confined spaces. Hence, in this study, we have fabricated grippers with varying design parameters and experimentally verified the inner diameter in the initial state and the radius of curvature when pressurized. We fabricated grippers with varying stiffness of rubber sheets and constant-force springs, which are components of the gripper, and experimentally verified their shape. The results show that the radius of curvature increases with increasing stiffness of the inner rubber sheet and decreasing stiffness of the constant-force spring. Additionally, it has been confirmed that the effect of the outer rubber sheet stiffness is sufficiently small.

I. INTRODUCTION

In disaster sites, grasping irregularly shaped heavy objects is required, necessitating grippers with high shape adaptability. Thus, unlike conventional rigid grippers, the use of soft grippers with flexibility is expected. However, although various soft grippers have been developed [1] [2], their load capacities are small, making them difficult to utilize in disaster sites. For example, there are various soft grippers such as those with soft links and joints like human hands [3] [4], finger-type grippers made of soft materials [5] [6], and helical-wrapping grippers made of soft materials [7] [8], but they cannot grasp heavy objects. Accordingly, various soft grippers aimed at improving load capacity have also been developed. For instance, hollow cylindrical grippers envelop objects by inflation [9], with having a load capacity of 539 N. A gripper with a locking mechanism at its tip [10] structurally supports objects, having a load capacity of 1000 N. However, construction machine robots developed for use in disaster sites have load capacities of 4000 N for the one developed by Kim et al. [11] and 10,000 N for the one developed by Nishida et al. [12]. Therefore, the load

*This work was supported by JST [Moonshot R&D][Grant Number JPMJPS2032].

¹Hiroto Kodama, Hiroyuki Nabae, Gen Endo, and Koichi Suzumori are with the Department of Mechanical Engineering, Institute of Science Tokyo, 2-12-1 Ookayama, Meguro-ku, Tokyo 152-8550, Japan kodama.h.6638@m.isct.ac.jp

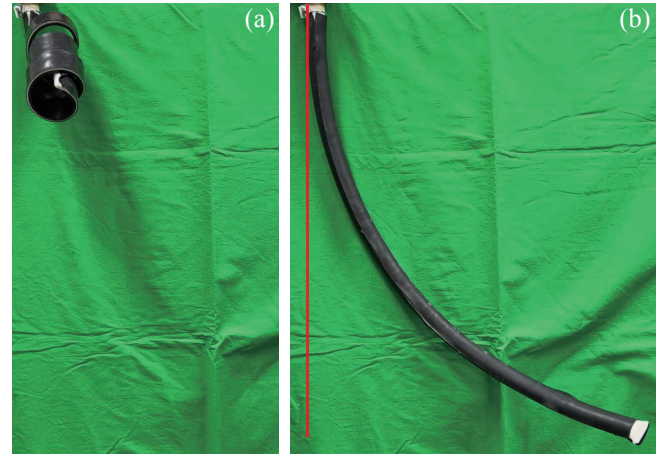


Fig. 1. Shape of Vine-Like, power soft gripper. (a). Initial state. (b). Pressurized.

capacity of soft grippers developed so far is insufficient to utilize them in disaster sites.

Hence, we focused on vine-type soft grippers [13] [14]. Although the load capacity of previously developed vine-type soft grippers is small, we thought that by wrapping around objects in a spiral manner, the contact area could be increased, thereby enhancing the load capacity. Based on this idea, we developed a vine-Like, power soft gripper [15] that wraps around objects in a helical manner, as shown in Fig. 1. This gripper consists of a fire hose with a spiral constant-force spring inserted. In its initial state, it is coiled in a spiral shape as shown in Fig. 1(a), and when air pressure is applied, it extends while increasing its radius of curvature as shown in Fig. 1(b). When depressurized, it rewinds to its initial state. When grasping an object, it approaches the target object with air pressure applied, and then wraps around the object by depressurized. This gripper wraps around objects due to the restoring force of the constant-force spring, but it can achieve high load capacity not by the spring’s restoring force, but by a significant increase in friction depending on the wrapped length, based on Euler’s belt theory. However, when using a single gripper, there are cases where the target object rotates and the gripper unwinds when lifting heavy objects. Thus, by using two grippers with different spiral directions, the rotation of the object can be canceled out, enabling the grasping of heavy objects. In addition, At present, it has been confirmed that it can grasp objects weighing at least 1660 N.

When air pressure is applied to the gripper, it currently does not extend in a straight line as indicated by the red

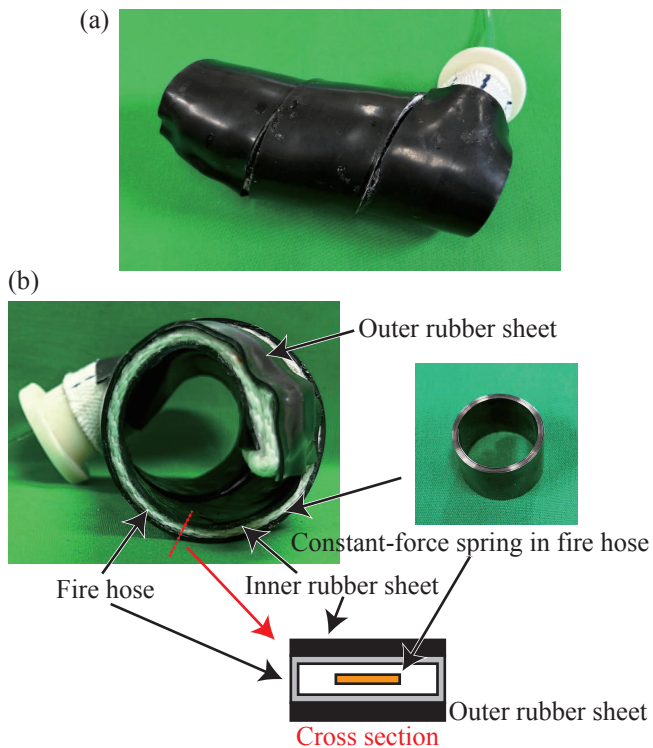


Fig. 2. Structure of the gripper. (a) Top view. (b) side view and cross section.

line in Fig. 1(b). As a result, the gripper's operating range that is its trajectory is restricted, limiting the objects that can be grasped and its use in narrow spaces when two grippers grasp. Regarding graspable objects, there are challenges such as insufficient opening at the tip when the width of the target object is large. However, the radius of curvature in the initial state also increases as the radius of curvature when pressurized increases. The smallest diameter of the object that the gripper can grasp becomes larger because the gripper grasps the object in the initial state when no pneumatic pressure is applied. For these reasons, the radius of curvature of this gripper in the initial state and when pneumatic pressure is applied is important. Accordingly, in this study, we fabricate grippers with varying design parameters and experimentally verify the inner diameter in the initial state, and the radius of curvature when air pressure is applied. This will clarify the effect of the design parameters on the radius of curvature toward extending the gripper in a straight line while keeping the radius of curvature small in the initial state.

The remainder of this paper is organized as follows. Section 2 describes the structure and components of the gripper, Section 3 describes an experiment to verify the effect of design parameters using the fabricated gripper, and Section 4 discusses the experimental results. And finally, Section 5 presents conclusion and future work.

II. STRUCTURE OF VINE-LIKE, POWER SOFT GRIPPER

This section describes the structure of the gripper and the characteristics of its component, the fire hose. Fig. 2(a)

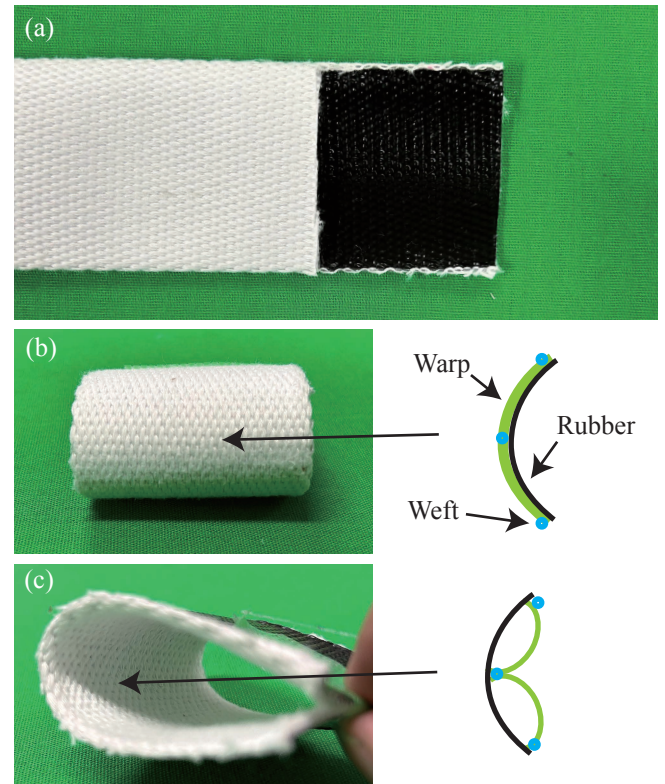


Fig. 3. Structure of fire hose. (a). Fire hose with part of it cut off. (b). Bend the side with the elastic inward and yarn condition. (c). Bend the side with the thread inward and yarn condition.

shows an overall view of the gripper and Fig. 2(b) shows a side view and cross section of the gripper. The gripper consists of an inner rubber sheet, a fire hose, a constant-force spring in the fire hose, and an outer rubber sheet. First, the inner rubber sheet is adhered to the fire hose kept straight. Second, the spring is inserted to the fire hose. Finally, the outer rubber sheet is bonded to the fire hose wrapped in a helical shape. The outer rubber sheet is adhered to the gripper to enable the gripper to rewind in a helical manner during the depressurization process. The inner rubber sheet is bonded to the gripper to ensure that the gripper rewinds without folding when depressurized.

Next, the fire hose used for the gripper is described. Fig. 3(a) shows a fire hose with a part of one side cut off. The fire hose is made by weft and warp yarns woven into a cylindrical shape and coated with melted rubber on the inside. The warp threads are pulled when the fire hose is bent with the rubber side inward as shown in Fig. 3(b), and the warp threads are loosened when the fire hose is bent with the yarn side inward as shown in Fig. 3(c). Therefore, the stiffness of the fire hose changes depending on the direction of bending. When the gripper bends, the inside of the fire hose is bent with the yarn side inward, and the outside of the fire hose is bent with the rubber side inward. However, the warp does not loosen because the rubber sheets are adhered to both sides of the fire hose. Hence, the difference in bending stiffness between the inside and outside of the

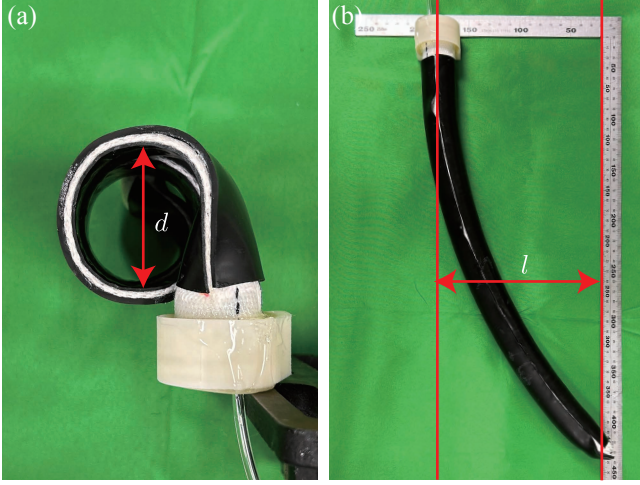


Fig. 4. Measurement position. (a). Inner diameter of gripper in the initial state. (b). Distance l when pneumatic pressure is applied.

TABLE I
DESIGN PARAMETERS OF GRIPPER

	t_{ro} [mm]	t_{ri} [mm]	t_s [mm]
1	1	1	0.3
2	2	1	0.3
3	3	1	0.3
4	1	3	0.3
5	1	5	0.3
6	1	1	0.13
7	1	1	0.2

gripper is considered to be determined by the rubber sheet, regardless of the fire hose.

III. EXPERIMENTAL VERIFICATION OF DESIGN PARAMETERS' EFFECT

In this section, the effects of design parameters on the inner diameter of the gripper in the initial state, and the radius of curvature of the gripper when air pressure is applied are experimentally verified. The design parameters include the stiffness of the fire hose, inner rubber sheet, outer rubber sheet, and constant-force spring. Here, the stiffness of the inner rubber sheet, outer rubber sheet, and constant-force spring are changed, whose stiffness can be easily changed. In this experiment, the inner diameter d in the initial state and the distance l from the center axis of the gripper root to the tip of gripper when pneumatic pressure was applied up to 0.4 MPa were measured as shown in Fig. 4(a)(b). For measurement convenience, the inner diameter was calculated by measuring the outer diameter and subtracting the thickness of the gripper. The table I shows the values of the design parameters of the fabricated gripper. These were selected based on parameters of the gripper in the previous study [15].

Fig. 5 shows change of inner diameter d and Fig. 5(a)(b)(c) shows when the thickness of the outer rubber sheet t_{ro} , the inner rubber sheet t_{ri} , and the spring t_{spring} is changed, respectively. Fig. 6 shows change of the distance l and

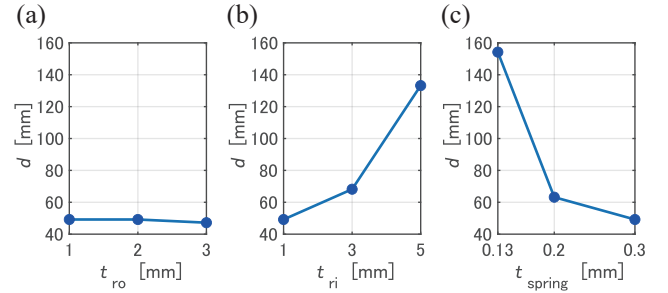


Fig. 5. Change of inner diameter d . (a). When the thickness of the outer rubber sheet t_{ro} is changed. (b). When the thickness of the inner rubber sheet t_{ri} is changed. (c). When the thickness of the spring t_{spring} is changed.

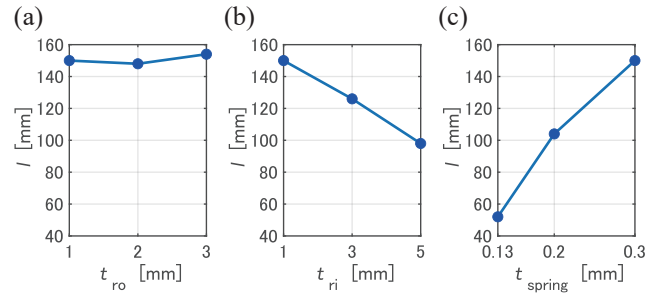


Fig. 6. Change of the distance l . (a). When the thickness of the outer rubber sheet t_{ro} is changed. (b). When the thickness of the inner rubber sheet t_{ri} is changed. (c). When the thickness of the spring t_{spring} is changed.

Fig. 6(a)(b)(c) shows when the thickness of the outer rubber sheet t_{ro} , the inner rubber sheet t_{ri} , and the spring t_{spring} is changed, respectively. A smaller distance means a larger radius of curvature. It was confirmed that the inner diameter and radius of curvature hardly changed when the thickness of the outer rubber sheet was changed. In addition, it was confirmed that the inner diameter and radius of curvature become larger when the thickness of the inner rubber sheet increased or the thickness of the spring decreased.

IV. DISCUSSION

We discuss the effect of design parameters on the inner diameter of the gripper in the initial state, and the radius of curvature of the gripper when air pressure is applied from the results obtained from the experiments in Section 3. For simplicity, we consider the inner diameter to be the radius of curvature.

First, the effect of the spring is considered. The radius of curvature increases as the thickness of the constant-force spring decreases. This is considered to be because, when a constant-force spring is regarded as a curved beam, the thinner the constant-force spring is, the smaller the amount of increase in the strain energy of the constant-force spring with respect to the increase in the radius of curvature. The bending strain energy U of a curved beam is expressed as follows.

$$U = \frac{1}{2}EI \left(\frac{1}{\rho} - \frac{1}{\rho_0} \right)^2 l \quad (1)$$

where ρ is the radius of curvature, ρ_0 is the radius of

curvature in the initial state, E is the modulus of longitudinal elasticity, I is the moment of inertia, l is the length, and EI is the stiffness. The equation (1) shows that the strain energy of a curved beam increases with increasing the radius of curvature. Because I becomes smaller as the constant-force spring becomes thinner, the amount of increase in strain energy of the constant-force spring with increasing radius of curvature becomes smaller. Thus, the radius of curvature at which the potential energy of the gripper reaches a minimum value increases, and the principle of minimum potential energy leads to a larger radius of curvature. From the above, it can be said that the stiffness of a constant-force spring should be small when considering the radius of curvature.

As the thickness of the inner rubber sheet is increased, the radius of curvature increases. This is because the amount of decrease in the strain energy of the inner rubber sheet with respect to the increase in the radius of curvature becomes larger as the thickness of the inner rubber sheet becomes thicker. Considering the rubber sheet as a beam, the strain energy of the rubber sheet U is expressed as follows.

$$U = \frac{1}{2}EI \left(\frac{1}{\rho}\right)^2 l + \frac{1}{2}EA\varepsilon^2 l \quad (2)$$

where A is the cross-sectional area, ε is the strain. The first term is the bending strain energy, and the second term is the tension or compression strain energy. The inner rubber sheet is adhered to the inside of the gripper at the same length as the fire hose. Hence, when air pressure is applied to the gripper, it attempts to return to original length. In other words, the strain decreases as the radius of curvature increases. Accordingly, the equation (2) shows that the bending and tension strain energy of the inner rubber sheet decreases with increasing radius of curvature. When a rubber sheet is thicker, I and A are larger, so the amount of decrease in strain energy of the rubber sheet with increasing radius of curvature is larger. Therefore, the radius of curvature at which the potential energy of the gripper reaches a minimum value increases, and the principle of minimum potential energy leads to a larger radius of curvature. From the above, it can be said that a thick inner rubber sheet is suitable for increasing the radius of curvature.

The radius of curvature hardly changed when the thickness of the outer rubber sheet was changed. The reason for this is thought to be that the change in compressive and bending strain energy of the outer rubber sheet relative to the radius of curvature changes only by the same amount even if the rubber sheet is thicker. The strain energy is expressed in the same way equation (2) when the rubber sheet is considered as a beam. However, unlike with the inner rubber sheet, the outer rubber sheet is longer than the length of the fire hose because it is adhered in a helical shape. Hence, when the gripper is pressurized, the outer rubber sheet is subjected to compression. In other words, the strain increases as the radius of curvature increases. Thus, the equation 2 shows that when the radius of curvature increases, the bending strain energy decreases, and the compression strain energy increases.

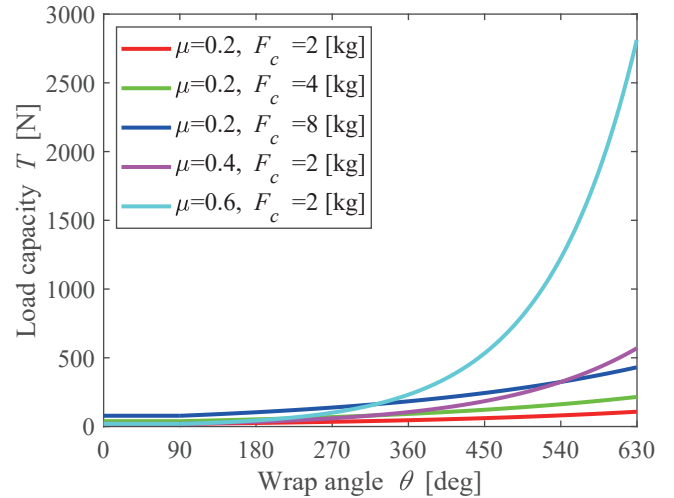


Fig. 7. Load capacities when changing the coefficient of static friction and the rated force of a constant-force spring.

When the rubber sheet is thickened, both the amount of decrease in bending strain energy and the amount of increase in compression strain energy become larger because A and I become larger. Considering that the increase in the amount of decrease in bending strain energy and the decrease in the amount of increase in compression strain energy are roughly equivalent, the change in strain energy relative to the radius of curvature before thickening the rubber sheet and after thickening should be approximately the same. A similar result is obtained when the radius of curvature is reduced, only the direction of change is reversed. In other words, the radius of curvature at which the gripper's potential energy reaches its minimum value hardly changes as the rubber sheet thickens. Based on the principle of minimum potential energy, it can be inferred that the radius of curvature remains almost unchanged.

When the inner rubber sheet thickness is 3 mm, the inner diameter is larger than when the spring thickness is 0.2 mm, but the radius of curvature when pneumatic pressure is applied is smaller. On the other hand, when the inner rubber sheet thickness is 5 mm, the inner diameter is smaller than when the spring thickness is 0.13 mm, and the radius of curvature is also smaller when pneumatic pressure is applied. This difference is considered to be caused by the change in the cross-section of the fire hose and rubber sheet between the initial state and when air pressure is applied. From this, it is considered that an optimal combination of the inner rubber sheet and spring thickness exists to decrease the inner diameter in the initial state and to increase the radius of curvature when pneumatic pressure is applied. The radius of curvature can be increased by thinning the constant-force spring, but in that case, the rated force of the spring becomes smaller and the load capacity of the gripper becomes smaller. This decrease in the load capacity can be prevented by increasing the coefficient of friction of the inner rubber sheet. When the gripper is wrapped around a cylindrical object, the load capacity $T(\theta)$ of the gripper with respect to the

wrap angle θ , which is the angle of the helical wrapping, is estimated as follows [15].

When $\theta \leq \pi/2$,

$$T(\theta) = F_c \quad (3)$$

When $\theta > \pi/2$,

$$T(\theta) = -\frac{F_c \lambda_2}{\lambda_1 - \lambda_2} \exp(\lambda_1 \theta) + \frac{F_c \lambda_1}{\lambda_1 - \lambda_2} \exp(\lambda_2 \theta) \quad (4)$$

where R and r are the radius of curvature of object and gripper, F_c is rated force of constant-force spring, μ is coefficient of static friction between the gripper and the object, and λ_1 and λ_2 are as

$$\lambda_1 = \frac{-R + \sqrt{R^2 + 4\mu^2(R-r)r}}{2\mu(R-r)} \quad (5)$$

$$\lambda_2 = \frac{-R - \sqrt{R^2 + 4\mu^2(R-r)r}}{2\mu(R-r)} \quad (6)$$

Fig.7 shows the effect of the static friction coefficient is larger than the effect of the rated force of the constant-force spring when the wrap angle is certain large from equations (3),(4). Accordingly, the decrease in the load capacity can be prevented by increasing the coefficient of friction of the inner rubber sheet when the rated force of a constant-force spring is decreased.

The radius of curvature can be increased by thickening the inner rubber sheet, but in that case, the gripper may not rewind due to its own weight. Therefore, nitrile rubber was used in this paper, but urethane rubber with a high modulus of elasticity and similar density is considered suitable.

V. CONCLUSIONS

In this study, the effects of design parameters on the shape of vine-Like, power soft gripper in the initial state and when air pressure is applied were verified. Specifically, grippers with different design parameters were fabricated, and the effects of the design parameters on the radius of curvature were experimentally verified. The experimental results showed that the radius of curvature increased with increasing the stiffness of the inner rubber sheet and decreasing the stiffness of the constant-force spring. In addition, it is confirmed that the effect of the outer rubber sheet stiffness is sufficiently small.

Future work will focus on determining the optimum inner rubber sheet and spring thickness to increase the radius of curvature while decreasing the inner diameter in the initial state by modeling the radius of curvature of the gripper.

REFERENCES

- [1] J. Shintake, V. Cacucciolo, D. Floreano, and H. Shea, "Soft robotic grippers," *Advanced Materials*, vol. 30, no. 29, p. 1707035, 2018. [Online]. Available: <https://onlinelibrary.wiley.com/doi/abs/10.1002/adma.201707035>
- [2] L. Zhou, L. Ren, Y. Chen, S. Niu, Z. Han, and L. Ren, "Bio-inspired soft grippers based on impactive gripping," *Advanced Science*, vol. 8, no. 9, p. 2002017, 2021. [Online]. Available: <https://onlinelibrary.wiley.com/doi/abs/10.1002/advs.202002017>
- [3] A. K. Mishra, E. Del Dottore, A. Sadeghi, A. Mondini, and B. Mazzolai, "Simba: Tendon-driven modular continuum arm with soft reconfigurable gripper," *Frontiers in Robotics and AI*, vol. 4, 2017. [Online]. Available: <https://www.frontiersin.org/articles/10.3389/frobt.2017.00004>

- [4] M. Manti, T. Hassan, G. Passetti, N. D'Elia, C. Laschi, and M. Cianchetti, "A bioinspired soft robotic gripper for adaptable and effective grasping," *Soft Robotics*, vol. 2, no. 3, pp. 107–116, 2015. [Online]. Available: <https://doi.org/10.1089/soro.2015.0009>
- [5] K. Suzumori, S. Iikura, and H. Tanaka, "Development of flexible microactuator and its applications to robotic mechanisms," in *Proceedings. 1991 IEEE International Conference on Robotics and Automation*. Los Alamitos, CA, USA: IEEE Computer Society, apr 1991, pp. 1622,1623,1624,1625,1626,1627. [Online]. Available: <https://doi.ieeecomputersociety.org/10.1109/ROBOT.1991.131850>
- [6] B. S. Homberg, R. K. Katzschmann, M. R. Dogar, and D. Rus, "Haptic identification of objects using a modular soft robotic gripper," in *2015 IEEE/RSJ International Conference on Intelligent Robots and Systems (IROS)*, 2015, pp. 1698–1705.
- [7] W. Wang, C. Li, M. Cho, and S.-H. Ahn, "Soft tendril-inspired grippers: Shape morphing of programmable polymer-paper bilayer composites," *ACS Applied Materials & Interfaces*, vol. 10, no. 12, pp. 10419–10427, Mar 2018. [Online]. Available: <https://doi.org/10.1021/acsami.7b18079>
- [8] M. Yang, L. P. Cooper, N. Liu, X. Wang, and M. P. Fok, "Twining plant inspired pneumatic soft robotic spiral gripper with a fiber optic twisting sensor," *Opt. Express*, vol. 28, no. 23, pp. 35 158–35 167, Nov 2020. [Online]. Available: <https://opg.optica.org/oe/abstract.cfm?URI=oe-28-23-35158>
- [9] D. Sui, T. Wang, S. Zhao, X. Zhang, J. Zhao, and Y. Zhu, "An enveloping soft gripper with high-load carrying capacity: Design, characterization and application," *IEEE Robotics and Automation Letters*, vol. 7, no. 1, pp. 373–380, 2022.
- [10] H. Li, P. Zhou, S. Zhang, J. Yao, and Y. Zhao, "A high-load bioinspired soft gripper with force booster fingers," *Mechanism and Machine Theory*, vol. 177, p. 105048, 2022. [Online]. Available: <https://www.sciencedirect.com/science/article/pii/S0094114X22002956>
- [11] J. T. Kim, S. Park, S. Han, J. Kim, H. Kim, Y.-H. Choi, J. Seo, S. Chon, J. Kim, and J. Cho, "Development of disaster-responding special-purpose machinery: Results of experiments," *Journal of Field Robotics*, vol. 39, no. 6, pp. 783–804, 2022. [Online]. Available: <https://onlinelibrary.wiley.com/doi/abs/10.1002/rob.22078>
- [12] T. Nishida, H. Koga, Y. Fuchikawa, Y. Kitayama, S. Kurogi, and Y. Arimura, "Development of pilot assistance system with stereo vision for robot manipulation," in *2006 SICE-ICASE International Joint Conference*, 2006, pp. 2675–2680.
- [13] R. V. Martinez, J. L. Branch, C. R. Fish, L. Jin, R. F. Shepherd, R. M. D. Nunes, Z. Suo, and G. M. Whitesides, "Robotic tentacles with three-dimensional mobility based on flexible elastomers," *Advanced Materials*, vol. 25, no. 2, pp. 205–212, 2013. [Online]. Available: <https://onlinelibrary.wiley.com/doi/abs/10.1002/adma.201203002>
- [14] H. Amase, Y. Nishioka, and T. Yasuda, "Mechanism and basic characteristics of a helical inflatable gripper," in *2015 IEEE International Conference on Mechatronics and Automation (ICMA)*, 2015, pp. 2559–2564.
- [15] H. Kodama, T. Ide, F. Yunhao, H. Nabae, and K. Suzumori, "Vine-like, power soft gripper based on euler's belt theory," *IEEE Robotics and Automation Letters*, vol. 9, no. 4, pp. 3108–3115, 2024.